INTERNATIONAL DESIGN CONFERENCE – DESIGN 2024
https://doi.org/10.1017/pds.2024.184

An analytic cost model for bound metal deposition

Mikhailo Sartini, Iacopo Bianchi, Alessio Vita, Michele Germani and Marco Mandolini ✉

Università Politecnica delle Marche, Italy

✉ m.mandolini@staff.univpm.it

Abstract

Metal material extrusion is a family of metal additive manufacturing that includes atomic diffusion additive manufacturing (ADAM) and bound metal deposition (BMD). In the literature, there are just a few cost models for ADAM and no one for BMD. The paper presents an analytic cost model for BMD. It considers the entire process: pre-processing, printing and post-processing. The total manufacturing cost is split into material, machine, labour, energy and consumables items. The cost model validation on a 3D-printed part determined an accuracy of 98%.

Keywords: design costing, additive manufacturing, cost estimation, metal material extrusion, design to cost

1. Introduction and literature review

Metal Additive Manufacturing (MAM) is a 3D printing technology with the most significant impact across various industries (e.g., aerospace, biomedical, energy) (Armstrong *et al.* 2022). According to ASTM/ISO 52900:2021 (ISO ASTM Standard 2021), MAM is divided into these categories: material extrusion (MEX), material jetting (MJ), binder jetting (BJ), powder bed fusion (PBF), directed energy deposition (DED), sheet lamination (SL), and vat polymerisation (VPP). PBF is the most widespread process technology since its maturity and high accuracy (Mandolini *et al.* 2022), covering 85% of the MAM market (AMPOWER GmbH & Co 2020). On the other hand, PBF machines are complex and expensive.
Recently, metal MEX (M-MEX) has been attracting attention for the following advantages: low cost (e.g., desktop systems), simple equipment (user-friendliness), fewer potential hazards (e.g., absence of metal powder loss), limited power source (compared to PBF or DED) and increased environmental sustainability (Suwanpreecha and Manonukul 2022; Bianchi *et al.* 2022). On the other hand, the main disadvantage of M-MEX concerns the filament (e.g., selection of binder types) and its production process (e.g., suitable mixing procedure). It is requested to guarantee high quality of the filament to guarantee the final shape, size, dimension and properties of 3D printed parts (Suwanpreecha and Manonukul 2022).
M-MEX, also called mFFF (metal fused filament fabrication, (Bankapalli *et al.* 2023)), FDMet (fused deposition of metals, (Bankapalli *et al.* 2023)), metal FDM (Ramazani and Kami 2022), MF3 (metal fused filament fabrication, (Singh *et al.* 2020)), is inspired by MIM (metal injection moulding) and FFF (Fused Filament Fabrication) (Bankapalli *et al.* 2023). The rapid growth is because this technology benefits from the substantial investment made by FFF and MIM. Indeed, material MEX is similar to MIM (concerning the overall process), apart from the way the green part is manufactured. M-MEX can create parts with properties close (or identical) to MIM. Regarding design freedom, metal MEX is more appealing as it eliminates moulds.
The M-MEX feedstock comprises metal powder and a polymeric binder (Figure 1). The 3D object (green part) is created by extruding the feedstock onto a build platform. Debinding is required to remove some of the polymeric material. Sintering is the last process that completely densifies the part by

combining the metal powders and burning the leftover polymeric binder. The material density after sintering is around 98% (Desktop Metal Inc. 2024a), lower than PBF.
Depending on the feeding system of the printer, the M-MEX process can be classified into three types: (i) screw-based, (ii) plunger-based, and (iii) filament-based types (Suwanpreecha and Manonukul 2022). The plunger-based system utilises bar feedstock to feed to the nozzle of the plunger system. This solution is adopted by Desktop Metal and is called "bound deposition modelling" (BMD) (Desktop Metal 2023). The most common and extensively utilised M-MEX technique is filament-based, also called "atomic diffusion additive manufacturing" (ADAM), which is proposed by Markforged (Markforged 2023).

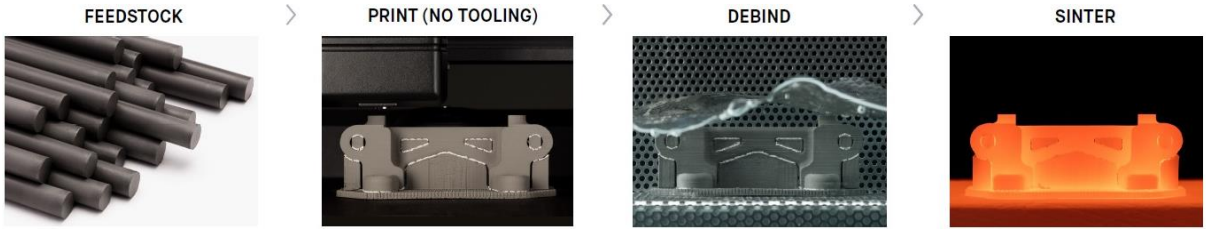

Figure 1. Bound Metal Deposition™ flow chart (Desktop Metal Inc 2024b)

The cost competitiveness of additive manufacturing versus traditional processes is often evaluated to suggest to design engineers when AM is cost-effective (Sæterbø and Solvang 2023). Such analyses are based on models for cost estimation. The literature on cost analysis has extensively examined other MAM technologies, such as PBF and DED. There are a lot of analytical methods available, such as (Rickenbacher *et al.* 2013), (Baumers *et al.* 2012), (Mandolini *et al.* 2022), (Mandolini *et al.* 2023).
Since its novelty and lower adoption, M-MEX (also intending mFFF, MF3, FDMet and metalFDM) was not investigated as the other MAM technologies. The most recent cost model was presented by (Sæterbø and Solvang 2023). The study is focused on the ADAM version of M-MEX, the one adopted by Markforged. The authors conceived an analytic model considering the production process (i.e., printing, debinding and sintering). A comparison with CNC machining determined the competitiveness of ADAM. Another analytic cost model was previously proposed by (Deboer *et al.* 2021). The authors developed their cost models for ADAM processes for two commercially available AM machines, Ultimaker S5 and Markforged Metal X. The model accounts for machine, material, and processing costs. Process parameters are explicit, thus making the model not ready for use. Another cost model is proposed by (Quarto and Giardini 2023). The model accounts for the activities required to set up the equipment and produce the part. The debinding and sintering phases are not considered because the authors' main goal was to compare M-MEX with MIM, which shares these activities. This study does not explicitly present process parameters to replicate the model. Furthermore, it is not evident which M-MEX technology is considered. A simple cost modelling for M-MEX was performed by (Tosto *et al.* 2021). The authors aimed to demonstrate that M-MEX has a solid potential to allow the printing of metal parts at a lower cost.
The scientific literature consists of a few analytic cost models for M-MEX. The models available often miss process parameters to replicate the calculation schema within a tool. Furthermore, the known cost models refer only to ADAM technology. Even if ADAM and BMD have a similar process (printing, debinding and sintering), the feedstock and the process parameters differ. To compare these technologies and evaluate the cost benefits of each one, it is essential to define a cost model specific to BMD. To the best of the authors' knowledge, there are no models for BMD. Thus, the paper aims to define an analytic cost model for MBD, which accounts for the printing, debinding and sintering phases. The cost breakdown considers material, labour, machine, consumable and energy costs.
After this introduction, section 2 presents the cost model's overall structure by listing the cost drivers. The model is broken down into pre-processing, build and post-processing phases following the process flow. Section 3 aims to validate the cost model by comparing this study's results with information obtained during physical experimentation.

2. The BMD cost model

The analytical cost model for BMD was obtained by reviewing and merging information in the literature and through the support provided by technical experts in this technology. BMD process guidelines, articles,

https://doi.org/10.1017/pds.2024.184 Published online by Cambridge University Press

handbooks, technical datasheets and the authors' direct use of the technology were considered to formulate the background of the entire printing process. From the information gathered and acquired, it was possible to define the main process parameters that characterise the time and cost of this printing process.
It is possible to divide the printing process for BMD into three main phases: pre-processing, build, and post-processing. The proposed analytical cost model defines analytical relationships for all three stages, contributing to the definition of the total process cost. According to (Mandolini *et al.* 2020), the total cost of each process phase can be defined as the sum of five cost items:

$$C_{Total} = C_{Material} + C_{Machine} + C_{Labour} + C_{Energy} + C_{Consumables} \quad (1)$$

Where $C_{Material}$ represents the material cost, $C_{Machine}$ machine cost, C_{Labour} labour cost, C_{Energy} energy cost and $C_{Consumables}$ consumables cost. Therefore, the total cost of the entire printing process is defined as the sum of the total costs of each stage.

2.1. Cost drivers

The use of the cost model passes through the inclusion of specific information as input. The provided data, denoted as cost drivers, pertains to the attributes of the component to be produced and the information employed in its production. The cost drivers related to the components' characteristics are the following: component size (size X, size Y, size Z), part volume, support volume, surface area to be supported, and material. The cost drivers associated with the process information in the production of the component are batch quantity (i.e., number of printed parts) and accuracy (print resolution). The latter assumes two values (high and low). Process parameters, such as layer thickness and nozzle diameter, depend on the accuracy. Thus, production time and cost are influenced by the accuracy.

2.2. Pre-processing phase

The pre-processing phase represents all the operations done by the technician to prepare the printing job. For this phase, labour is the only cost item considered.

$$C_{labour} = \frac{\left[\left(\left(T_{set-up} * n_{job}\right) + T_{nesting}\right) * C_{operator\ hourly\ rate}\right]}{n_{components}} \quad (2)$$

T_{set-up} is ideally the time to load the material cartridge, position and remove the build plate, and remove the components from the build plate. From a practical point of view, only the handling of the build plate and the removal of the components are considered. The material cartridge can be used for numerous print jobs; its replacement time is only a few seconds. It can, therefore, be neglected. $T_{nesting}$ is the time to prepare the print job. It represents the time spent by the operator to optimise the print space, orient the part, generate the supports, slicing and loading the print file into the printer. Note that the nesting time is only considered for the first printing job since the nesting is the same. Only the setup time is considered for production batches that involve more than one printing job. $C_{operator\ hourly\ rate}$ is the operator hourly rate. n_{job} is the number of printing jobs required to produce the required batch quantity ($n_{components}$).

2.3. Build phase

The build phase represents the time spent by the machine to print the job. To estimate this phase, all the cost items are considered except labour cost (no actions required by the operator) and consumables cost. The material cost is a crucial element that significantly impacts the cost model.

$$C_{material} = \{\left[\left(V_{component} + V_{support}\right) * (1 + \%_{sh.})^3\right] * \rho_{material} * C_{mat.uni.cost} + \left(V_{interface} * \rho_{interf.} * C_{interf.uni.cost}\right)\} \quad (3)$$

$V_{component}$ and $V_{support}$ represent the volume of the component and the support structure, respectively. By multiplying these parameters with density, the respective masses are obtained.
Sintering activity during post-processing densifies the component, reducing its size (17-22 %, depending on the material (Desktop Metal 2023). $\%_{sh.}$ represents how much to increase the size to account for the subsequent densification (Shrinkage Percentage). $V_{interface}$ is the amount of ceramic material to be

https://doi.org/10.1017/pds.2024.184 Published online by Cambridge University Press

interposed between component and support structures. This technology consists of two extruders. The first is to print the part with its supports, and the second is to deposit the ceramic material. The latter, during printing, is deposited between the part and the support structures to facilitate subsequent support removal operation and ensure proper sintering. It depends on the Surface Area to be supported and the layer thickness of the deposited ceramic material. $C_{mat.uni.cost}$ and $C_{interf.uni.cost}$ represent the material unitary cost and ceramic unitary cost respectively. $\rho_{material}$ and $\rho_{interface}$ represent the material density of the component and ceramic density respectively.
The machine cost is a further cost item of primary importance. It is linked to the 3D printer's hourly rate and the build time.

$$C_{machine} = T_{Build} * C_{machine\ hourly\ rate} \tag{4}$$

According to (Ruffo *et al.* 2006), the machine's hourly rate ($C_{machine\ hourly\ rate}$) is function of the hourly rate of deprecation, production overhead and maintenance. The calculation of this parameter further depends on specific parameters like purchasing cost, annual working time, building yearly rent rate, building area, depreciation time, load factor, maintenance cost and discount factor.
T_{Build} represents the time for the model building operation.

$$T_{Build} = \left[\frac{(S_{component}+S_{support}+S_{interface})}{v_{machine}}\right] \tag{5}$$

where the $S_{component}$, $S_{support}$ and $S_{interface}$ are the average paths the extruder performs to build the component, support structures, and interface layers, respectively. $v_{machine}$ represents the average speed at which the extruder moves.
In detail, the average path of the extruder $P_{component}$ can be defined with the following relationship (the relationships remain the same for the support structures considering their respective volume):

$$S_{component} = A_{equivalent}/D_{nozzle} \tag{6}$$

where D_{nozzle} is the nozzle diameter as a function of accuracy. $A_{equivalent}$ represents the surface area equivalent to the model to be made. It is defined as the ratio between the volume of the component considering the shrinkage percentage ($V_{component} * (1 + \%_{sh.})^3$) and the layer thickness as a function of accuracy ($l_{thickness}$). Equation (6) can be directly used for the interface material path. In this case, however, the surface area to be supported is applied instead of the equivalent area.
The energy cost represents the electricity used by the printer during the build phase.

$$C_{Energy} = C_{energy\ unitary\ cost} * P_{machine} * T_{Build} \tag{7}$$

It depends on the energy unitary cost of the electricity ($C_{energy\ unitary\ cost}$), the power absorbed by the machine during the build phase ($P_{machine}$) and the build time.
It is worth noting that the proposed equations define the manufacturing cost for an individual component. It is possible to obtain the total cost of the print job by providing the total volume (components and supports) and the total path (components, supports and interface) resulting from the components into the equations. In the case of a print job composed of different components, it is possible to obtain the unit cost of each part by allocating the total cost as a function of the total volume (component and media) of the considered component.

2.4. Post-processing phase

The process ends with post-processing operations. Two activities are typically performed after the printing stage: debinding and sintering. For the first one, the part is placed in the debinder, where a significant portion of the primary binder is removed by chemical dissolution. In contrast, the remaining binder helps the part retain its shape. Considering the first relationship previously introduced, the items considered for this activity are material cost, machine cost, labour cost and energy cost.

$$C_{material} = \left(\frac{V_{reagent}}{n_{components}}\right) * C_{reag.uni.cost} \tag{8}$$

https://doi.org/10.1017/pds.2024.184 Published online by Cambridge University Press

In this case, the material cost depends on the amount of reagent introduced into the debinder ($V_{reagent}$) and its unit cost ($C_{reag.uni.cost}$).

$$C_{machine} = \left(\frac{T_{debinding}}{n_{components}}\right) * C_{debinder\ hourly\ rate} \quad (9)$$

The machine cost is a function of the hourly cost of the debinder ($C_{debinder\ hourly\ rate}$) and the processing time ($T_{debinding}$) of this step (usually fixed depending on the material processed). The machine hourly rate is obtained considering the parameters defined in Chapter 2.3.

$$C_{labour} = \left(\frac{T_{set-up_{deb.}}}{n_{components}}\right) * C_{operator\ hourly\ rate} \quad (10)$$

Labour cost is related to the time spent by the operator to start the machine, fill it with reagent, place the components inside and extract them ($T_{set-up_{deb.}}$) and its unitary cost. Finally, energy cost is assessed through equation (7). In this case, the power the machine absorbs is referred to as the debinder machine and the time the components come in contact with the reagent. The cost is divided by the number of parts placed in the debinder.
Regarding the sintering activity, parts are placed in the furnace and heated to temperatures near melting. The remaining binder is released, and metal particles fuse, causing the component to densify up to 99%. Starting from equation (1), the cost items considered are machine cost, labour cost, energy cost, and consumables cost.

$$C_{machine} = \left(\frac{T_{sintering}}{n_{components}}\right) * C_{furnace\ hourly\ rate} \quad (11)$$

Machine cost depends on the furnace's hourly rate ($C_{furnace\ hourly\ rate}$) and heating time ($T_{sintering}$). Note that the sintering time is closely related to the component's material and whether debinding is performed.

$$C_{labour} = \left(\frac{T_{set-up_{sint.}}}{n_{components}}\right) * C_{operator\ hourly\ rate} \quad (12)$$

The labour cost is related to placing and extracting the components from the furnace ($T_{set-up_{sint.}}$). As for the debinding phase, starting from equation (7), the energy cost for this operation depends on the power absorbed by the furnace, the energy unitary cost and the sintering time. The cost is divided by the number of components placed in the furnace.

$$C_{consumables} = \left(\frac{V_{unitary\ inert\ gas} * T_{sintering}}{n_{components}}\right) * C_{inert\ gas\ unitary\ cost} \quad (13)$$

The furnace uses a gas to inertise the chamber. The amount of gas used is a function of sintering time and the volume of gas introduced per unit time. Therefore, the cost will depend on the amount of gas used to inert the chamber at each cycle and its unit cost ($C_{inert\ gas\ unitary\ cost}$).

3. Cost model validation

A tensile test specimen was printed to evaluate and validate the relationships presented within the cost model. The test specimen was then used for different works to evaluate its mechanical properties (Bellezze *et al.* 2023), (Forcellese *et al.* 2022) and environmental impact (Bianchi *et al.* 2022). The latter shows the numerical data of the entire printing process used to compare the values of the expressions introduced. In detail, the component (Figure 2) is printed with the Studio System printer from Desktop Metal.

Figure 2. Test specimen

https://doi.org/10.1017/pds.2024.184 Published online by Cambridge University Press

3.1. Geometrical and process information

Table 1 shows the geometric information of the component, provided as input to the cost model, and the process information with which the product is manufactured. The volume of components already considers the shrinkage rate of 18.75%.

Table 1. Geometrical and process information

Component		Process	
Size X [mm]	196	Printer	Studio System
Size Y [mm]	30	Part Material	17-4 PH Stainless Steel
Size Z [mm]	5	Support Material	17-4 PH Stainless Steel
Part Volume [mm^3]	13420	Interface Material	Ceramic
Support Volume [mm^3]	11630	Reagent	Trans-Dichlorethylene
Surface area to be supported [mm^2]	3769.7	Debinder	Debinder Studio System
Batch quantity	1	Furnace	Furnace Studio System
Quality	High	Inert gas	Argon

3.2. Cost model calculation

In this sub-section, the costs for each process phase are calculated and compared. The comparison is made in detail by entering actual process parameters into the cost model (such as build time or weight of material used) to calculate the cost of the different cost items of each phase. These real parameters are those recorded after the actual printing of the specimen. After that, the estimated parameters from the model are used to obtain the cost and compare. Costs obtained from real data are defined as actual costs, while costs obtained from model estimates are denoted as estimated costs. Table 2 provides information for calculating the parameters used to get the actual and estimated costs.

Table 2. Basic parameters

*Hourly rates obtained considering a Load Factor of 57%, which corresponds to 4,993 working hours per year (Lindemann *et al.* 2012; Ruffo *et al.* 2006). **Measured parameters

Material		Studio System		Debinder Studio System		Furnace Studio System	
Material Unitary Cost [€/kg]	100	Acquisition Cost [€]	150,000	Acquisition Cost [€]	40,000	Acquisition Cost [€]	60,000
Ceramic Unitary Cost [€/kg]	100	Machine Hourly Rate [€/h]	10.30*	Machine Hourly Rate [€/h]	4.10*	Machine Hourly Rate [€/h]	5.25*
Material Density [g/cm^3]	5.01 (Desktop Metal Inc. 2024a)	Power Consumption [W]	1500 (Desktop Metal Inc 2024a)	Power Consumption [W]	2000 (Desktop Metal Inc. 2024b)	Power Consumption [W]	6240 (Desktop Metal Inc. 2024c)
Ceramic Density [g/cm^3]	2.07 (Desktop Metal Inc. 2024a)	Layer thickness [mm]	0.1 (Bianchi *et al.* 2022), (Forcellese *et al.* 2022)	Reagent Unitary Cost [€/kg]	5	Unitary Gas Consumption [l/h]	0.005**
		Nozzle Diameter [mm]	0.25 (Bianchi *et al.* 2022)	Debinding time [h]	13 (Bianchi *et al.* 2022)	Sintering Time [h]	41 (Bianchi *et al.* 2022)
		Printing speed [mm/s]	30 (Bellezze *et al.* 2023)	Operator Hourly Rate [€/h]		30	
				Energy Unitary Cost [€/kWh]		0.5	

https://doi.org/10.1017/pds.2024.184 Published online by Cambridge University Press

Data without reference are obtained by looking at technical information of the machines and purchase invoices.

3.2.1. Pre-processing phase

Considering equation (2), the cost related to the pre-processing phase is defined. In this case, the times are the same for actual and estimated costs. Manual operations of this type have many variables and are, therefore, difficult to assess with a report. The times were monitored during the printing phase of the component.

$$T_{set-up}= 6 \text{ min}; T_{nesting}= 10 \text{ min}; n_{job}=1; n_{components}=1 \quad (14)$$

$$C_{pre-processing\ phase} = C_{labour} = \frac{\left[\left((T_{set-up}*n_{job})+T_{nesting}\right) * C_{operator\ hourly\ rate}\right]}{n_{components}} = 8\ € \quad (15)$$

3.2.2. Build Phase

Regarding the build phase, the main parameters estimated by the model are the printing time and the amount of material used (Table 3). The following values are obtained using the equations in Chapter 2.3 and the information in Table 1 for the component and Table 2 for the process. Information on material consumption was obtained directly from the printing software for actual values. Energy consumption was measured using measuring instruments.

Table 3. Cost model validation for the build phase

Process parameter	Estimated value	Actual value	Deviation [%]
Material weight [g]	101.45	121.4	-16%
Print time [h]	10.42	11	-5%
Ceramic weight [g]	1.2	1.55	-23%
Material Cost [€]	10.32	15.35	-33%
Machine Cost [€]	107.32	113.3	-5%
Energy Cost [€]	7.72	8.25	-6%

3.2.3. Post-processing phase

The times and parameters for the two post-processing phases are fixed as a function of the material processed (Table 4). Therefore, there are no differences at this stage either.

Table 4. Cost model validation for the post-processing phase

Post-processing phase	Process parameter	Estimated value	Actual value	Deviation [%]
Debinding	Reagent Volume [kg]	0.00155	0.00155	0%
	Set up time [min]	10	10	0%
	Material cost [€]	0.075	0.075	0%
	Machine cost [€]	53.33	53.33	0%
	Labour Cost [€]	5.00	5.00	0%
	Energy Cost [€]	13.00	13.00	0%
Sintering	Machine cost [€]	215.25	215.25	0%
	Energy Cost [€]	127.92	127.92	0%
	Consumables Cost [€]	2.16	2.16	0%

3.2.4. Total Manufacturing cost

This section compares the actual and estimated total manufacturing costs (Table 5). The deviation is 2%. Thus, the accuracy is 98%.

https://doi.org/10.1017/pds.2024.184 Published online by Cambridge University Press

Table 5. Total manufacturing cost validation

Process phase	Cost item	Estimated Cost [€]	Actual Cost [€]	Deviation [%]
Pre-processing	Labour	22.50	22.50	0%
Build	Material	10.32	15.35	-33%
	Machine	107.32	113.3	-5%
	Energy	7.72	8.25	-6%
Debinding	Material	0.075	0.075	0%
	Machine	53.33	53.33	0%
	Labour	5.00	5.00	0%
	Energy	13.00	13.00	0%
Sintering	Machine	215.25	215.25	0%
	Energy	127.92	127.92	0%
	Consumables	2.16	2.16	0%
	Total	564.60	576.14	**-2%**

4. Conclusions

The paper presented an analytical cost model for the total manufacturing cost estimation of the bound metal deposition metal process. The model considers the entire workflow, from pre-processing to post-processing (i.e., debinding and sintering). The preliminary validation has been carried out on a tensile test specimen printed through the Studio System printer from Desktop Metal. The accuracy of the total manufacturing cost is 98%.

For the future, the cost model must be validated by considering other parts with different shapes, dimensions, and materials. Manual activities should be estimated considering a learning curve typical of additive manufacturing processes. Moreover, the cost model should be extended to consider the atomic diffusion additive manufacturing process, for example, that used by Markforged. The improved model will allow designers and engineers to compare the two widespread commercial technologies concerning M-MEX (Desktop Metal and Markforged). Furthermore, from the analytic cost model presented here, it is interesting to build up a parametric cost model (e.g., €/cm^3) to be used during the preliminary design phases to evaluate if and when to use M-MEX processes.

References

AMPOWER GmbH & Co (2020) AMPOWER Report 2020.

Armstrong, M, Mehrabi, H, and Naveed, N (2022) An overview of modern metal additive manufacturing technology. Journal of Manufacturing Processes, 84(November), 1001–1029. https://dx.doi.org/10.1016/j.jmapro.2022.10.060.

Bankapalli, NK, Gupta, V, Saxena, P, Bajpai, A, Lahoda, C, and Polte, J (2023) Filament fabrication and subsequent additive manufacturing, debinding, and sintering for extrusion-based metal additive manufacturing and their applications: A review. Composites Part B: Engineering, 264(May), 110915. https://dx.doi.org/10.1016/j.compositesb.2023.110915.

Baumers, M, Tuck, C, Wildman, R, Ashcroft, I, Rosamond, E, and Hague, R (2012) Combined build-time, energy consumption and cost estimation for direct metal laser sintering. 23rd Annual International Solid Freeform Fabrication Symposium - An Additive Manufacturing Conference, SFF 2012, (January), 932–944.

Bellezze, T, Forcellese, A, Forcellese, P, Mancia, T, and Simoncini, M (2023) Effect of printing orientation on mechanical properties of components in stainless steel obtained using the Bound Metal Deposition technology. Procedia CIRP, 118, 694–698. https://dx.doi.org/10.1016/j.procir.2023.06.119.

Bianchi, I, Di Pompeo, V, Mancia, T, Pieralisi, M, and Vita, A (2022) Environmental impacts assessment of Bound Metal Deposition 3D printing process for stainless steel. Procedia CIRP, 105(March), 386–391. https://dx.doi.org/10.1016/j.procir.2022.02.064.

Deboer, B, Diba, F, and Hosseini, SA (2021) Design And Development Of A Cost Calculator For Additive Manufacturing. https://dx.doi.org/10.32393/csme.2021.167.

Desktop Metal (2023) Deep Dive: Bound Metal Deposition (BMD). Retrieved November 13, 2023, from https://www.desktopmetal.com/resources/deep-dive-bmd

https://doi.org/10.1017/pds.2024.184 Published online by Cambridge University Press

Desktop Metal Inc. (2024a) 17-4 PH stainless steel. Retrieved February 13, 2024, from https://www.desktopmetal.com/uploads/Studio-MDS-17-4-PH-stainless-steel.pdf
Desktop Metal Inc. (2024b) Debinder technical data. Retrieved February 13, 2024, from https://cdn.webshopapp.com/shops/24440/files/222339395/studio-debinder-data-sheet.pdf
Desktop Metal Inc. (2024c) Furnace Specifications. Retrieved February 13, 2024, from https://www.desktopmetal.com/uploads/BMD-SPC-Furnace1.6-210910.pdf
Desktop Metal Inc (2024a) Studio SystemTM 2 Printer Specifications. Retrieved February 13, 2024, from https://www.desktopmetal.com/uploads/20230407_BMD-SPC-Printer.pdf
Desktop Metal Inc (2024b) Understanding Bound Metal Deposition. Strength of Studio System parts.
Forcellese, P, Mancia, T, Simoncini, M, and Bellezze, T (2022) Investigation on Corrosion Resistance Properties of 17-4 PH Bound Metal Deposition As-Sintered Specimens with Different Build-Up Orientations. Metals, 12(4), 588. https://dx.doi.org/10.3390/met12040588.
ISO ASTM Standard (2021) ASTM/ISO 52900:2021. Additive manufacturing General principles Fundamentals and vocabulary.
Lindemann, C, Jahnke, U, Moi, M, and Koch, R (2012) Analyzing Product Lifecycle Costs for a Better Understanding of Cost Drivers in Additive Manufacturing. In SFF Symposium, International Solid Freeform Fabrication Symposium, Vol. 23, , 177–189.
Mandolini, M, Campi, F, Favi, C, Germani, M, and Raffaeli, R (2020) A framework for analytical cost estimation of mechanical components based on manufacturing knowledge representation. The International Journal of Advanced Manufacturing Technology. https://dx.doi.org/10.1007/s00170-020-05068-5.
Mandolini, M, Sartini, M, Favi, C, and Germani, M (2022) Cost Sensitivity Analysis for Laser Powder Bed Fusion. Proceedings of the Design Society, 2, 1411–1420. https://dx.doi.org/10.1017/pds.2022.143.
Mandolini, M, Sartini, M, Favi, C, and Germani, M (2023) An Analytical Cost Model for Laser-Directed Energy Deposition (L-DED). In Advances on Mechanics, Design Engineering and Manufacturing IV, , 993–1004. https://dx.doi.org/10.1007/978-3-031-15928-2_87.
Markforged (2023) What is Atomic Diffusion Additive Manufacturing (ADAM)? Retrieved November 13, 2023, from https://markforged.com/it/resources/learn/3d-printing-basics/3d-printing-processes/what-is-atomic-diffusion-additive-manufacturing-adam
Quarto, M, and Giardini, C (2023) Additive manufacturing of metal filament: when it can replace metal injection moulding. Progress in Additive Manufacturing, 8(3), 561–570. https://dx.doi.org/10.1007/s40964-022-00348-w.
Ramazani, H, and Kami, A (2022) Metal FDM, a new extrusion-based additive manufacturing technology for manufacturing of metallic parts: a review. Progress in Additive Manufacturing, 7(4), 609–626. https://dx.doi.org/10.1007/s40964-021-00250-x.
Rickenbacher, L, Spierings, A, and Wegener, K (2013) An integrated cost-model for selective laser melting (SLM). Rapid Prototyping Journal, 19(3), 208–214. https://dx.doi.org/10.1108/13552541311312201.
Ruffo, M, Tuck, C, and Hague, R (2006) Cost estimation for rapid manufacturing - Laser sintering production for low to medium volumes. Proceedings of the Institution of Mechanical Engineers, Part B: Journal of Engineering Manufacture, 220(9), 1417–1427. https://dx.doi.org/10.1243/09544054JEM517.
Sæterbø, M, and Solvang, WD (2023) Evaluating the cost competitiveness of metal additive manufacturing – A case study with metal material extrusion. CIRP Journal of Manufacturing Science and Technology, 45, 113–124. https://dx.doi.org/10.1016/j.cirpj.2023.06.005.
Singh, P, Balla, VK, Tofangchi, A, Atre, S V., and Kate, KH (2020) Printability studies of Ti-6Al-4V by metal fused filament fabrication (MF3). International Journal of Refractory Metals and Hard Materials, 91(March), 105249. https://dx.doi.org/10.1016/j.ijrmhm.2020.105249.
Suwanpreecha, C, and Manonukul, A (2022) A Review on Material Extrusion Additive Manufacturing of Metal and How It Compares with Metal Injection Moulding. Metals, 12(3). https://dx.doi.org/10.3390/met12030429.
Tosto, C, Tirillò, J, Sarasini, F, and Cicala, G (2021) Hybrid metal/polymer filaments for fused filament fabrication (FFF) to print metal parts. Applied Sciences (Switzerland), 11(4), 1. https://dx.doi.org/10.3390/app11041444.

https://doi.org/10.1017/pds.2024.184 Published online by Cambridge University Press

https://doi.org/10.1017/pds.2024.184 Published online by Cambridge University Press